Thesis Progression Report

Anatole Verhaegen

July 5, 2015

Contents

Nomenclature

ρ_m linear mass density

$\rho_{m_{booster}}$ linear mass density of the booster

$\rho_{m_{dart}}$ linear mass density of the dart

E_i Young modulus of beam i

F_i external force along z-axis applied on node i

G center of gravity

$I_{G,y,i}$ or I_i second moment of area of beam i

$I_{G,y_{booster}}$ second moment of area of the booster about the neutral axis along the y-axis

$I_{G,y_{dart}}$ second moment of area of the dart about the neutral axis along the y-axis

$I_{G,y}$ second moment of area about the neutral axis along the y-axis

L missile length

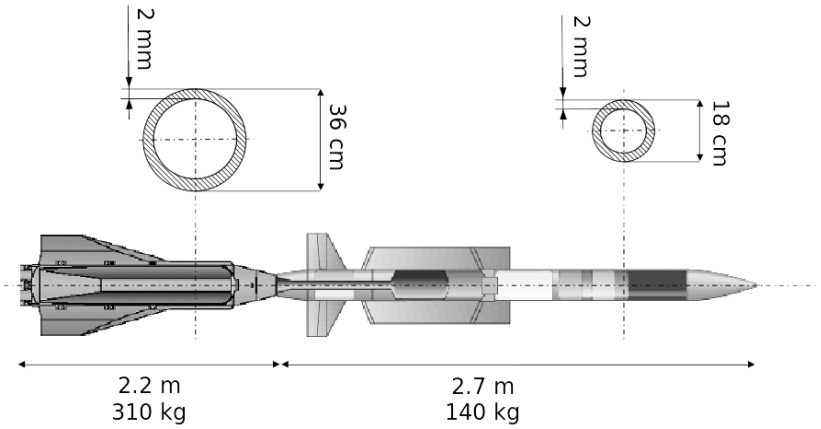

Figure 1: ASTER-30 Dimensions

l	length of an element beam
m	missile mass
m_i	mass of node i
$M_{y,i}$	external moment along y-axis applied on node i
n	number of nodes
E	longitudinal Young modulus of the missile

1 Structural Model

1.1 From continuous to discrete

ASTER-30 length is 4.9 m and the largest diameter is 0.36 m on the booster so the missile can be considered as a beam with variable cross section. Euler-Bernoulli beam theory is suitable here because higher order models like Timoshenko beam theory would bring additive complexity and precision that are not needed for this study. Therefore sections rotational inertia and shear deformation are neglected. For the purpose of this study, only bending along y-axis is considered so deformations of the missile are contained in the zx-plane.

During the acceleration phase, ASTER-30 is composed of two parts: the booster and the dart. Both of them can be modeled as cylindrical pipes. The booster section has a diameter of 36 cm and the dart is 18 cm wide. The skin thickness[1] of the missile is 2 mm. These dimensions are illustrated in Figure 1.

[1]Estimated from the natural frequency of the 1st bending mode at 20Hz

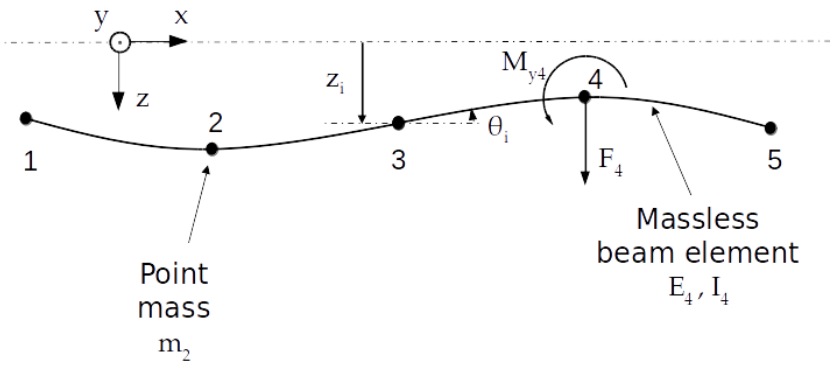

Figure 2: Lumped Element Model of a Beam (5 nodes)

The material used for the missile is assumed to be 30% carbon fibres composites and unidirectional along the longitudinal axis. The Young modulus along the x-axis is $E = 180\,GPa$ for such a material. The second moment of area at the neutral axis along y-axis for a cylindrical section is:

$$I_{G,y} = \pi \frac{D^4 - (D - 2\,e)^4}{64}$$

with D and e the external diameter and thickness of the pipe. Thus, the second moment of area for the booster and the dart are :

$$\begin{cases} I_{G,y_{booster}} & = 3.60 \cdot 10^{-5}\, m^4 \\ I_{G,y_{dart}} & = 4.43 \cdot 10^{-6}\, m^4 \end{cases}$$

It is assumed that the missile mass is equally distributed in the dart and in the booster therefore the linear mass density ρ_m is uniform in the booster, and uniform in the dart:

$$\begin{cases} \rho_{m_{booster}} & = 140.9\, kg.m^{-1} \\ \rho_{m_{dart}} & = 51.9\, kg.m - 1 \end{cases}$$

It is necessary to discretize the body in order be able to conduct a state-space representation and simulations. To reach this goal, the mathematical model of the structure is designed using a lumped element model illustrated in Figure 2.

Geometry The missile is longitudinaly discretized in n nodes evenly spaced by the beams length $l = \frac{L}{n-1}$. The nodes i and $i+1$ are linked together by a massless Euler-Bernoulli beam i. Let z_i, $\dot{z}_i$ and $\ddot{z}_i$ be respectively the displacement, speed and acceleration of node i along the z-axis. θ_i, $\dot{\theta}_i$ and $\ddot{\theta}_i$ are respectively the pitch angle, pitch rate and pitch acceleration of the beams at the junction node i.

To determine the number of nodes needed, we can consider looking at the natural frequencies of the beam converging as n grows. On Figure 3, first structural mode

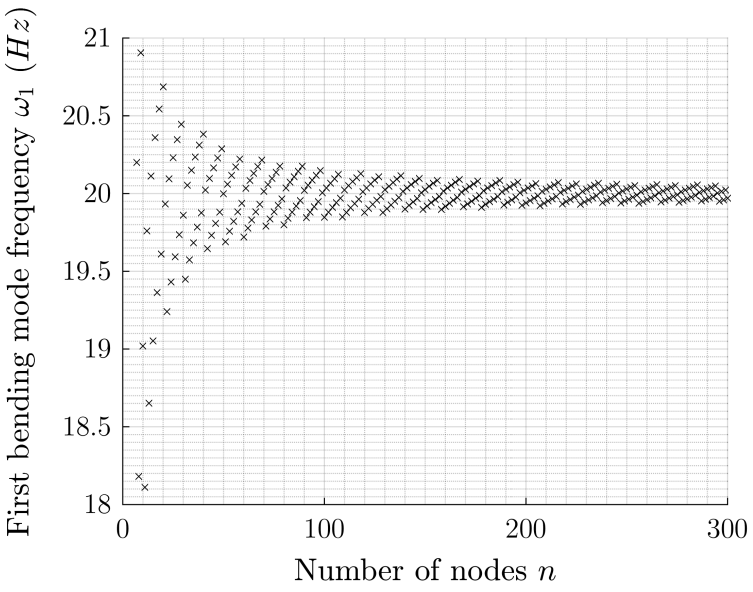

Figure 3: Computed First Mode Natural Frequency

frequencies have been computed[2] for n varying between 7 and 300. The frequency converges when n increases. Eventually $n = 100$ is a good choice to minimize the number of nodes for computational efficiency and having an acceptable accuracy on natural frequencies. Indeed, at about $n = 100$, the frequency oscillates between $19.85\,Hz$ and $20.15\,Hz$ which corresponds to $1.5\,\%$ of variation. It is worth noting that the uncertainty on the real first mode frequency is 5 to $10\,\%$ so with $n = 100$, the first mode frequency can be said as converged.

Mass and stiffness Each node $i \in [\![1, n]\!]$ has a point mass m_i that is the mass of the section from $x = (i - \frac{3}{2})\, l$ to $x = (i - \frac{1}{2})\, l$. Thus the mass is conserved during the discretization : $\sum_{i=1}^{n} m_i = m$. The Euler-Bernoulli beam i has a Young modulus E_i and the second moment of area at neutral axis passing through G and along y-axis $I_{G,y,i}$. For readability purposes, $I_{G,y,i}$ will be noted I_i but the reader must be carefull not to confuse it with a rotational inertia, generally noted J in this paper.

The different structural parameters of the body are summarized in Figure 4 for $n = 100$. It is clear that the booster is stiffer and heavier than the dart.

External efforts On each node i, an external force F_i along the z-axis and an external moment $M_{y,i}$ along the y-axis are applied.

[2]The method to do so will be explained later.

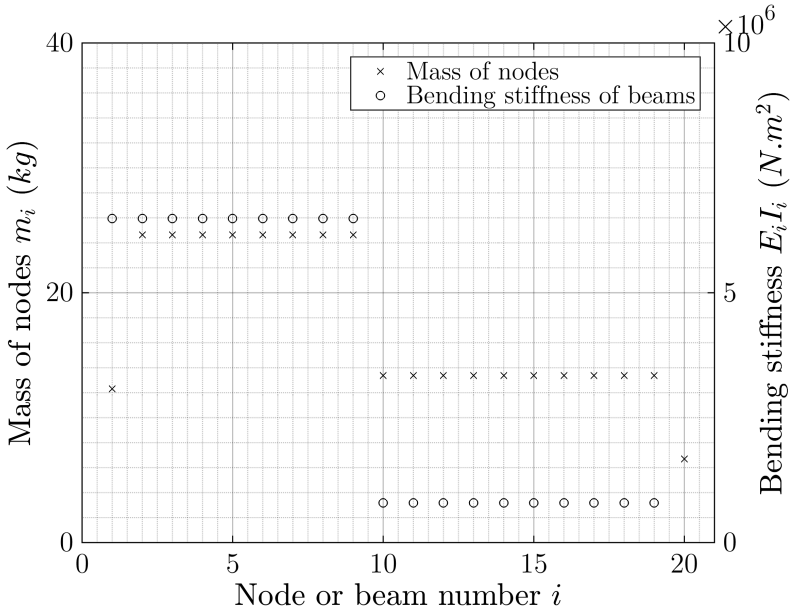

Figure 4: Summary of Structural Parameters for 20 Nodes

1.2 Second-Order Structural Model

1.2.1 Nodal Model

To generate a second-order structural model, Prentis and Leckie's method [3] will be used. This finite element model can be fully characterized by the following second-order structural equation:

$$M' \ddot{u} + D' \dot{u} + K' u = F' \tag{1}$$

- $u = \begin{bmatrix} z_1 \\ \vdots \\ z_n \\ \theta_1 \\ \vdots \\ \theta_n \end{bmatrix}$ is the displacement vector

- $F' = \begin{bmatrix} F_1 \\ \vdots \\ F_n \\ M_{y,1} \\ \vdots \\ M_{y,n} \end{bmatrix}$ is the external efforts matrix

- M' is the mass matrix of this system : $M' = \begin{bmatrix} M & 0_{n\times n} \\ 0_{n\times n} & J_y \end{bmatrix}$. M and J_y are diagonal matrices containing nodes masses and rotational inertias about the y-axis.
- K' and D' are the stiffness and damping matrices of this system.

K' can be divided in four sub-matrices $K' = \begin{bmatrix} K_{11} & K_{12} \\ K_{21} & K_{22} \end{bmatrix}$. In a static situation where $\ddot{u}$ and $\dot{u}$ are zero, the equation 1 becomes :

$$K'\,u = F' \tag{2}$$

Thus

$$\begin{bmatrix} K_{11} & K_{12} \\ K_{21} & K_{22} \end{bmatrix} \begin{bmatrix} z \\ \theta \end{bmatrix} = \begin{bmatrix} F \\ M_y \end{bmatrix}$$

Finding K' To derive this matrix, one can **consider only two nodes i and $i+1$** linked with the beam i. The equation2 is simplified to:

$$\begin{bmatrix} k_{11,i} & k_{12,i} \\ k_{21,i} & k_{22,i} \end{bmatrix} \begin{bmatrix} z_i \\ z_{i+1} \\ \theta_i \\ \theta_{i+1} \end{bmatrix} = \begin{bmatrix} F_i \\ F_{i+1} \\ M_{y,i} \\ M_{y,i+1} \end{bmatrix}$$

Four cases are considered and illustrated in Figure 5:

	z_i	z_{i+1}	θ_i	θ_{i+1}
Case 1	1	0	0	0
Case 2	0	1	0	0
Case 3	0	0	1	0
Case 4	0	0	0	1

The forces and moments applied to the beam are F_i, F_{i+1}, $M_{y,i}$ and $M_{y,i+1}$. The equilibrium between external efforts on the beam gives the two equations (forces and moments at node i):

$$F_i + F_{i+1} = 0 \tag{3}$$

$$M_{y,i} + M_{y,i+1} - l \cdot F_{i+1} = 0 \tag{4}$$

Using beam theory, the deformation and efforts are linked with the equation

$$E_i\, I_i\, \frac{\partial^2 z}{\partial x^2}(x) = -M_y(x) \tag{5}$$

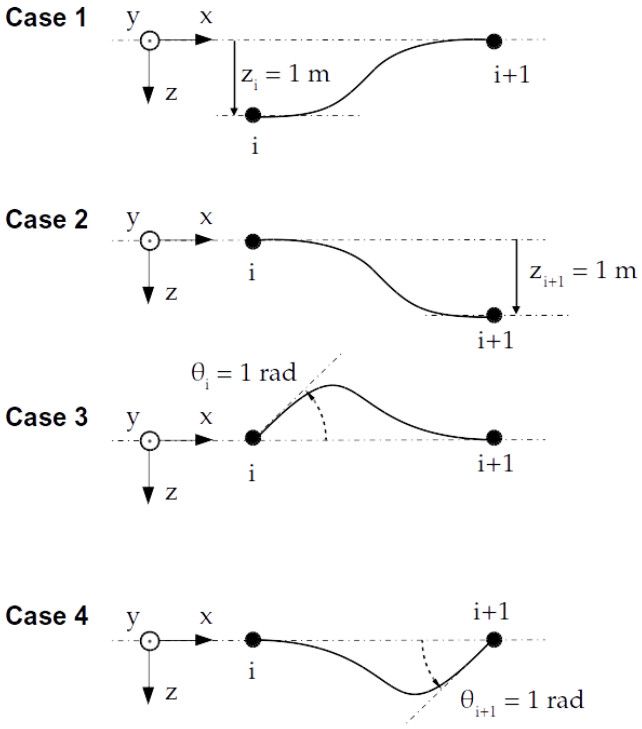

Figure 5: Elementary Cases for Two Nodes

where and $M_y(x) = M_{y,i+1} - (l - x)\, F_{i+1}$ are local young modulus, second moment of area and pitching moment at abscissa x [3]. For readability purposes, $E_i\, I_i$ will now be noted EI_i. This yields after integration and double integration

$$EI_i\theta(x) = -\frac{1}{2}x^2\, F_{i+1} + x\, (-M_{y,i+1} + l\, F_{i+1}) + A \tag{6}$$

$$EI_i z(x) = -\frac{1}{6}x^3\, F_{i+1} + \frac{1}{2}x^2\, (-M_{y,i+1} + l\, F_{i+1}) + A\, x + B \tag{7}$$

with A and B integration constants.

The boundary conditions are

$$\begin{cases} \theta(0) &= \theta_i \\ \theta(l) &= \theta_{i+1} \\ z(0) &= z_i \\ z(l) &= z_i \end{cases} \tag{8}$$

Thus, the system of equations 3, 4, 6, 7 and 8 for each case 1 to 4 yields :

	Case 1	Case 2	Case 3	Case 4
F_i	$12\, EI_i/l^3$	$-12\, EI_i/l^3$	$-6\, EI_i/l^2$	$-6\, EI_i/l^2$
F_{i+1}	$-12\, EI_i/l^3$	$12\, EI_i/l^3$	$6\, EI_i/l^2$	$6\, EI_i/l^2$
$M_{y,i}$	$-6\, EI_i/l^2$	$6\, EI_i/l^2$	$4\, EI_i/l$	$2\, EI_i/l$
$M_{y,i+1}$	$-6\, EI_i/l^2$	$6\, EI_i/l^2$	$2\, EI_i/l$	$4\, EI_i/l$

thus $k_{11,i}$, $k_{12,i}$, $k_{21,i}$ and $k_{22,i}$ derived from the table above are

$$\begin{cases} k_{11,i} &= \frac{12\, EI_i}{l^3} \begin{bmatrix} 1 & -1 \\ -1 & 1 \end{bmatrix} \\ k_{12,i} = k_{21,i}^T &= \frac{6\, EI_i}{l^2} \begin{bmatrix} -1 & -1 \\ 1 & 1 \end{bmatrix} \\ k_{22,i} &= \frac{2\, EI_i}{l} \begin{bmatrix} 2 & 1 \\ 1 & 2 \end{bmatrix} \end{cases}$$

Now considering the complete missile, as the element beams are linked in serie, the matrices K_{11}, K_{12}, K_{21}, and K_{22} can be calculated by summing the matrices $k_{11,i}$, $k_{12,i}$, $k_{21,i}$ and $k_{22,i}$ on the diagonal as shown below for K_{11}:

[3] $x = 0$ at node i and $x = l$ and node $i + 1$

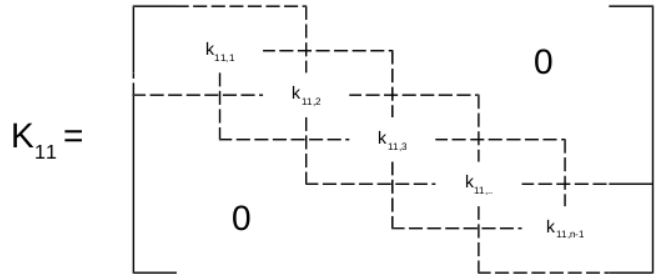

Thus, these matrices are

$$K_{11} = \frac{12}{l^3}\begin{bmatrix} EI_1 & -EI_1 & 0 & \cdots & 0 \\ -EI_1 & EI_1 + EI_2 & \ddots & \ddots & \vdots \\ 0 & \ddots & \ddots & \ddots & 0 \\ \vdots & \ddots & \ddots & EI_{n-2} + EI_{n-1} & -EI_{n-1} \\ 0 & \cdots & 0 & -EI_{n-1} & EI_{n-1} \end{bmatrix}$$

$$K_{12} = K_{21}^T = \frac{6}{l^2}\begin{bmatrix} -EI_1 & -EI_1 & 0 & \cdots & 0 \\ EI_1 & EI_1 - EI_2 & \ddots & \ddots & \vdots \\ 0 & \ddots & \ddots & \ddots & 0 \\ \vdots & \ddots & \ddots & EI_{n-2} - EI_{n-1} & -EI_{n-1} \\ 0 & \cdots & 0 & EI_{n-1} & EI_{n-1} \end{bmatrix}$$

$$K_{22} = \frac{2}{l}\begin{bmatrix} 2\,EI_1 & EI_1 & 0 & \cdots & 0 \\ EI_1 & 2\,EI_1 + 2\,EI_2 & \ddots & \ddots & \vdots \\ 0 & \ddots & \ddots & \ddots & 0 \\ \vdots & \ddots & \ddots & 2\,EI_{n-2} + 2\,EI_{n-1} & EI_{n-1} \\ 0 & \cdots & 0 & EI_{n-1} & 2\,EI_{n-1} \end{bmatrix}$$

It is worth noting that $K' = K'^T$ that can be explained by Maxwell-Betti reciprocal work theorem.

Simplified second-order structural model In this study, we assume that the pure external moments $M_{y,i}$ are negligeable when compared to moments created by the forces F_i. The missile is modeled as an Euler-Bernoulli beam, thus the local rotational inertias I_i are zero. The damping D' is very few for such flexible structures so it can be neglected for the next trick. With these hypotheses, the lower part of Equation 1 concerning rotational acceleration becomes :

$$0_{n\times 1}\,\ddot{\theta} + 0_{n\times 1}\dot{\theta} + K_{21}z + K_{22}\theta = 0_{n\times 1}$$

K_{22} is a symmetric tridiagonal matrix which invertibility can be proven by LU decomposition[1]. This leads to the important relation between z and θ:

$$\theta = -K_{22}^{-1}\, K_{21} z \tag{9}$$

This equation mean that the second part of u can be entirely determined from its first part. The upper part of the Equation 1 fully describes the structural system:

$$M\, \ddot{z} + D\, \dot{z} + (K_{11} - K_{12}K_{22}^{-1}K_{21})\, z = F$$

The stiffness matrix is then $K = K_{11} - K_{12}K_{22}^{-1}K_{21}$. One can verify that $K^T = K$.

The damping matrix is chosen proportionnal to K and set to damp the first structural mode to 1%. This gives $D = K/6000$. The second-order structural equation is as follows:

$$M\, \ddot{z} + D\, \dot{z} + K\, z = F \tag{10}$$

1.2.2 Modal Model

The triplet (M,D,K) is the nodal realization of the second-order structural model. A modal realization must be found to extract the flexible body modes from the structural model. The transformation of the nodal model is described in [2] and can be derived as follows.

Considering free vibrations without damping, the system being linear, the displacement vector will be $z = \phi e^{j\omega t}$ with ϕ constant thus $\ddot{z} = -\omega^2 \phi e^{j\omega t}$ and Equation 10 becomes:

$$(-\omega^2 M + K)\, \phi = 0 \tag{11}$$

Non-trivial solutions to Equation 11 (i.e. $\phi \neq 0$) exist if and only if

$$\det(-\omega^2 M + K) = 0$$

The solutions are the generalized eigen values $(\omega_1^2, \omega_2^2, ..., \omega_n^2)$ of the matrices K and M. $(\omega_1, \omega_2, ..., \omega_n)$ are the natural frequencies of the structure and the eigen vectors $(\phi_1, \phi_2, ..., \phi_n)$ are the natural modes also called modes shape.

In this particular study, the structure extremities are free hence the two first natural frequencies are $0\,Hz$ and the two first natural modes correspond to the rigid-body modes: z-axis translation and y-axis rotation. The natural frequencies and modes shape are renamed $(0, 0, \omega_1, \omega_2, ..., \omega_{n-2})$ and $(\phi_{0,1}, \phi_{0,2}, \phi_1, \phi_2, ..., \phi_{n-2})$.

The modes shape of the rigid-body and the first three bending modes are plotted in Figure 6. This figure shows that the dart is likely to bend more than the booster. Indeed, the front part of the missile is more flexible so it will bend more.

The natural frequencies for the first modes are summarized in Table 1.

Let $\Phi = [\phi_{0,1}\ \phi_{0,2}\ \phi_1\ \phi_2\ \ldots\ \phi_{n-2}]$ be the modal matrix and

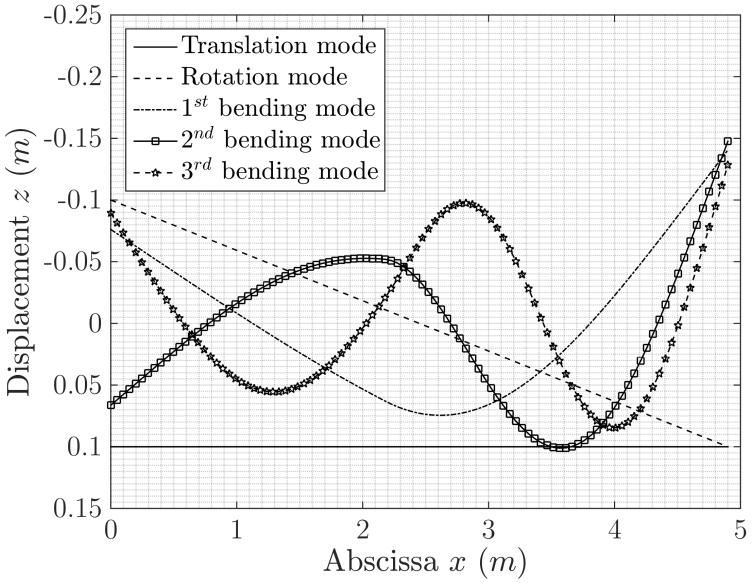

Figure 6: Modes Shape of ASTER-30

Mode	Frequency	
	(Hz)	$(rad.s^{-1})$
z translation mode	0	0
y rotation mode	0	0
1^{st} bending mode	20.0	125
2^{nd} bending mode	67.7	425
3^{rd} bending mode	139.7	877
4^{th} bending mode	213.9	1344
5^{th} bending mode	335.1	2106

Table 1: Natural Frequencies of Modes

$$\Omega = \begin{bmatrix} 0 & & & & \\ & 0 & & & 0 \\ & & \omega_1 & & \\ & & & \ddots & \\ 0 & & & & \omega_{n-2} \end{bmatrix}$$

be the matrix of natural frequencies.

Let z_m be the displacement vector of modes defined by $z = \Phi z_m$. The modal matrices of mass M_m, damping D_m and stiffness K_m are obtained as follows

$$M_m = \Phi^T M \Phi$$

$$D_m = \Phi^T D \Phi$$

$$K_m = \Phi^T K \Phi$$

The triplet (M_m,D_m,K_m) defines the second-order structural modal model of the missile. The equation 10 becomes:

$$M_m \, \ddot{z}_m + D_m \, \dot{z}_m + K_m \, z_m = \Phi^T F \tag{12}$$

1.2.3 Output equation

Three types of sensors are investigated in this paper to measure vibrations: strain gages, gyrometers and accelerometers. Their measurement can be represented by the output equation:

$$y = C_{oz} z + C_{ov} \dot{z} + D_o F \tag{13}$$

where y is a vector containing the measurement of all sensors.

It means that the signal measured by the sensors are a linear combination of the displacement of the nodes (matrix C_{oz}), their speed (matrix C_{ov}) and also a feedforward term D_o on the external forces applied on the nodes.

Gyrometer A gyrometer on node i measures $\dot{\theta}_i$, thus n gyrometers can be placed. Since q is often used to represent the pitch rate, this letter will be used for gyrometer output matrices. According to Equation 9, $\theta = K_{22}^{-1} K_{21} z$, therefore $\dot{\theta}_i = K_{22}^{-1} K_{21} \dot{z}$. This yields the output matrices

$$C_{ozq} = 0_{n \times n} \qquad C_{ovq} = K_{22}^{-1} K_{21} \qquad \text{and} \qquad D_{oq} = 0_{n \times n}$$

Accelerometer An accelerometer on node i measures $\ddot{z}_i$. The letter assigned to acceleration measurement will be a like "acceleration" and the measurement will be called a_z. With an accelerometer on each node, there are n accelerometers. In Equation 13, $\ddot{z}$ does not appear. But using the second-order structural equation 10:

$$\ddot{z} = -M^{-1}K\,z - M^{-1}D\,\dot{z} + F$$

thus

$$C_{oza} = -M^{-1}K \qquad C_{ova} = -M^{-1}D \qquad \text{and} \qquad D_{oa} = Id_n$$

Strain gage For a strain gage, a first order Taylor developpement to approximate the spatial derivative of $\theta(x)$ at node i will be conducted. This approximation cannot be made on nodes 1 and n therefore, only $n-2$ strain gages are considered. The letter used for this sensor is ε which is often assigned to strains.

The Euler-Bernoulli beam theory assumes that each section stays perpendicular to the neutral axis. The strain gages are placed on the upper side of the missile therefore, the local deformation at the surface is

$$\varepsilon(x) = -\frac{\partial\theta}{\partial x}\frac{D(x)}{2}$$

where $D(x)$ is the local missile diameter. It is worth noting that $\varepsilon(x)$ is positive when the strain gage is stretched and negative when it is compressed.

The partial derivative of θ with respect to x is approximated using a first order Taylor developpement at node $i \in [\![2, n-1]\!]$:

$$\frac{\partial\theta}{\partial x}(x_i) \simeq \frac{\theta_{i+1} - \theta_{i-1}}{2\,l}$$

thus

$$\varepsilon_i = \frac{-\theta_{i+1} + \theta_{i-1}}{2\,l}\,\frac{D_i}{2}$$

Let $\varepsilon = (\varepsilon_i)_{i\in[\![2,n-1]\!]}$, then the previous equation yields

$$\varepsilon = T_\varepsilon\theta$$

with

$$T_\varepsilon = \frac{1}{4\,l}\begin{bmatrix} D_2 & 0 & -D_2 & & & & & 0 \\ & D_3 & 0 & -D_3 & & & & \\ & & D_4 & 0 & -D_4 & & & \\ & & & \ddots & \ddots & \ddots & & \\ & & & & D_{n-2} & 0 & -D_{n-2} & \\ 0 & & & & & D_{n-1} & 0 & -D_{n-1} \end{bmatrix}$$

Finally, using Equation 9, the relation becomes

$$\varepsilon = T_\varepsilon K_{22}^{-1} K_{21} z$$

hence

$$C_{oz\varepsilon} = -T_\varepsilon K_{22}^{-1} K_{21} \qquad C_{ov\varepsilon} = 0_{(n-2)\times n} \qquad \text{and} \qquad D_{o\varepsilon} = 0_{(n-2)\times n}$$

Concatenation The output vector corresponding to the concatenation of all measurements is $y = \begin{bmatrix} \varepsilon \\ q \\ a_z \end{bmatrix}$.Therefore

$$C_{oz} = \begin{bmatrix} C_{oz\varepsilon} \\ C_{ozq} \\ C_{oza} \end{bmatrix} \qquad C_{ov} = \begin{bmatrix} C_{ov\varepsilon} \\ C_{ovq} \\ C_{ova} \end{bmatrix} \qquad \text{and} \qquad D_o = \begin{bmatrix} D_{o\varepsilon} \\ D_{oq} \\ D_{oa} \end{bmatrix}$$

Modal output matrix The Output Equation 13 will finally be

$$y = C_{oz}\Phi z_m + C_{ov}\Phi \dot{z}_m + D_o F$$

defining the modal equivalent of the output matrices :

$$y = C_{mz} z_m + C_{mv}\Phi \dot{z}_m + D_o F$$

with

$$\begin{cases} C_{mz} & = C_{oz}\Phi \\ C_{mv} & = C_{ov}\Phi \end{cases}$$

1.3 Rigid-body Modes Elimination

The second-order structural model and its output equation in there modal forms have been derived. However, the two rigid-body modes - translation and rotation - must be eliminated. Indeed, this Chapter aims at modeling only vibrations during the flight. The rigid-body dynamics modeled have not been derived using flight dynamics and must be suppressed to keep only vibrations dynamics.

The matrices M_m, D_m and K_m are diagonal meaning that there is no interaction between modes due to Equation 12. Thus, the equation can be simply truncated to get rid of the rigid-body modes by removing the first two rows of z_m and Φ. From now on,

Looking at the output Equation 13, truncated the rigid-body modes will remove pitch rate and strain measurement due to them. However, great care must be taken for the acceleration measurement.

1.4 State Space Model

References

[1] Moawwad El-Mikkawy and El-Desouky Rahmo. A new recursive algorithm for inverting general tridiagonal and anti-tridiagonal matrices. *Applied Mathematics and Computation*, 204(1):368–372, 2008.

[2] Wodek K Gawronski. *Dynamics and control of structures: A modal approach*. Springer Science & Business Media, 2004.

[3] James Martin Prentis and Frederick A Leckie. *Mechanical vibrations: an introduction to matrix methods*. Longmans, 1963.